

# HEAT TRANSFER OPTIMIZATION OF CROSS-FLOW OVER ASSEMBLIES OF BLUFF BODIES EMPLOYING CONSTRUCTAL PRINCIPLE

**Elizaldo Domingues dos Santos, edsantos@mecanica.ufrgs.br**

**Anderson Dall'Agnol, anderson.dall@yahoo.com.br**

**Adriane Prisco Petry, adrianep@mecanica.ufrgs.br**

Department of Mechanical Engineering

Universidade Federal do Rio Grande do Sul – Rua Sarmento Leite, 425 – Porto Alegre - RS

**Luiz Alberto Oliveira Rocha, laorochoa@gmail.com**

Escola de Engenharia

Universidade Federal do Rio Grande – Avenida Itália, km 8 – Rio Grande - RS

**Abstract.** *This paper applies Constructal Theory to maximize heat transfer rate in cross-flow over assemblies of square cylinders. The main goal is to obtain the optimal number of square cylinders or the optimal placement of each cylinder in the assembly to improve the heat exchange between the obstacle and the cross flow. The cross flow is steady, incompressible, laminar and two-dimensional. The conservation equations of mass, momentum and energy are solved using a commercial package based on finite volume method. The accuracy of the code is evaluated by simulations of flows over a square cylinder (bluff body) for low Reynolds numbers,  $Re = 60$  and  $160$ , and different Prandtl numbers,  $Pr = 1, 10$  and  $20$ . The results agree within 4% with those shown in the literature. The optimal configurations of assemblies of bluff bodies are obtained for several Reynolds numbers,  $Re = 60, 100$  and  $160$ , and Prandtl numbers,  $Pr = 0.1, 0.72, 1$  and  $10$ . These optimal configurations as function of Reynolds and Prandtl numbers are also compared with those available in the literature for an arrangement of circular cylinders. The optimal spacing between obstacles decreases monotonically as the Reynolds and Prandtl numbers increase.*

**Keywords:** *Constructal Theory, Bluff bodies in cross flow, Forced Convection, Optimization*

## 1. INTRODUCTION

This paper reports numerically the maximization of the heat transfer rate in cross-flow over a parallel arrange of square bluff-bodies. The optimization is conducted by applying Constructal design. According to this method “the flow geometry is malleable and it is deduced from a principle of global performance maximization subjected to global constraints” (Bejan, 1997; Bejan, 2000). This method is based on Constructal theory: “the view that flow configuration (geometry, design) can be reasoned on the basis of a principle of configuration, generation and evolution in time toward greater global flow access in systems that are free to morph” (Bejan and Lorente, 2008).

The many applications of Constructal theory to generate configuration in nature, and engineering has been appropriately reviewed by Bejan and Lorente (2006). This reference shows how natural configuration – river basins, turbulence, animal design, crack in solids, earth climate, etc, can be predicted by principle. The same principle can be applied in the engineering realm: packing of electronics, fuel cells, tree networks for transport of people, goods and information, etc.

More recently, Constructal theory has been used to optimize geometry configuration of heat sinks, cooling channels and micro-channels (Bello-Ochende *et al.*, 2007a; Bello-Ochende *et al.*, 2007b). The purpose of the first study was the maximization of the global thermal conductance, or the minimization of thermal resistance. To achieve this objective, the geometry configuration was submitted to the following global constraints: fixed volume of the heat-sink cooling channel and fixed total volume of the conducting solid. In the second work, a similar study was performed. However, other global constraints were evaluated for the optimization of the geometry: a fixed total elemental volume and a fixed axial length of the micro-channel heat sink. In both cases, Constructal theory led to the best geometry configurations. Besides that, Constructal theory has also been employed to increase the heat transfer rate in ducts by using wrinkled entrance regions (Bello-Ochende *et al.*, 2009) and to maximize the heat transfer in cross-flow over a parallel arrange of circular cylinders (Bello-Ochende *et al.*, 2005).

In this paper we apply Constructal design to optimize the heat transfer rate in cross-flow over a parallel arrange of square bluff-bodies. This kind of flow has been a subject of many engineering applications such as heat exchangers, solar heating systems and packing of electronics. According to Constructal design, the number of obstacles in the assembly is free to change subject to the constraint  $H/D_0$ , i.e. the ratio between the height of the assembly and the side length of the square obstacle, in the pursuit of maximal global performance. The global performance indicator is the global thermal conductance between the heated obstacles and the cross-flow. For simplicity and clarity, we consider two-dimensional configurations and take advantage of symmetry to build the computational domain.

## 2. NUMERICAL AND MATHEMATICAL MODELING

The analyzed physical problem consists of a cross-flow over a parallel arrange of square bluff-bodies, as can be seen in Fig. 1. In this study the fluid flow is heated by the square cylinder arrange subjected to a global restriction, which is given by the ratio between two fixed dimensions ( $H/D_0$ ), where  $H$  is the height of the assembly and  $D_0$  is the side length of the square cylinder. The optimization process aims to select the number of obstacles in the assembly, or the placement between each square cylinder ( $s_0$ ), such that the overall thermal conductance between the cylinder and the cross-flow is maximal. The flow is considered steady, incompressible, two-dimensional and laminar. Further, all the thermophysical properties are assumed constant.

The lower part of Fig. 1 illustrates the computational domain that characterizes this assembly. Though the flow over bluff bodies persists symmetric about the mid-plane up to about  $Re = 40$  (Sahu *et al.*, 2009), we assume that this non-symmetric behavior will not affect the evaluation of fluid dynamic and heat transfer parameters, such as drag and lift coefficients and Nusselt number. Therefore, it is simulated only half of channel formed between two obstacles. The same consideration was previously performed in the literature for simulations of cross-flow over circular cylinders arrange (Bello-Ochende and Bejan, 2005). The non-dimensional distance between the inlet plane and the front surface of the obstacles arrange ( $\tilde{L}_u$ ) and that between the rear surface of the cylinder and the exit plane ( $\tilde{L}_d$ ) were considered  $\tilde{L}_u = 8.5$  and  $\tilde{L}_d = 16.5$ , respectively (note that  $D_0$  is the length scale according to Eq. (5)). These values were chosen to avoid the influence of domain over on the heat transfer from the obstacle.

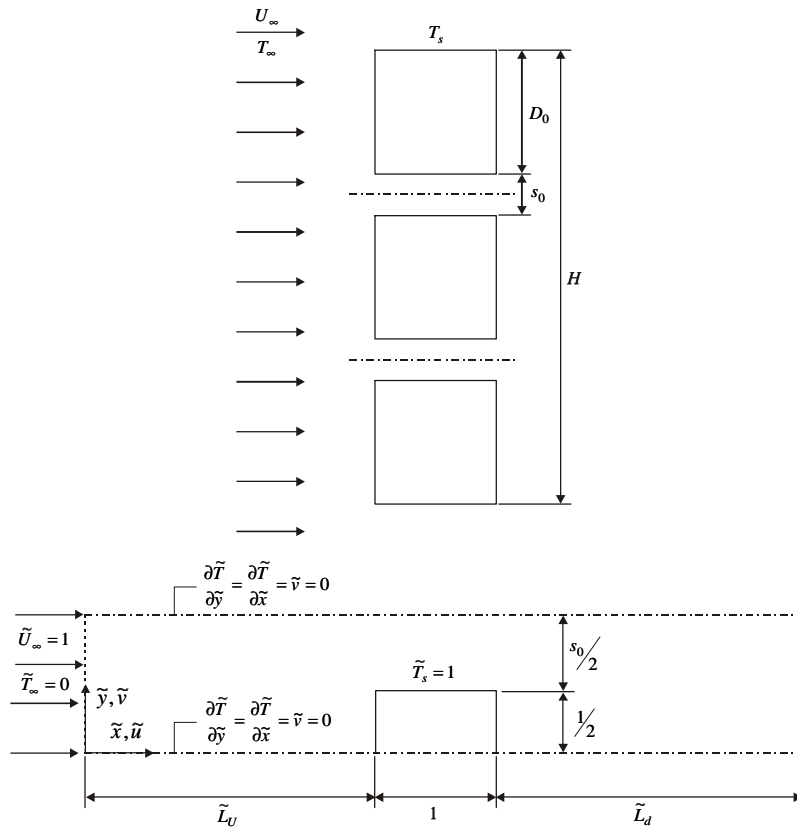


Figure 1. Parallel square cylinders arrange and the computational domain

The conservation equations of mass, momentum in  $x$  and  $y$  directions and energy, respectively, are given by (Bejan, 1994):

$$\frac{\partial u}{\partial x} + \frac{\partial v}{\partial y} = 0 \quad (1)$$

$$u \frac{\partial u}{\partial x} + v \frac{\partial u}{\partial y} = -\frac{1}{\rho} \frac{\partial P}{\partial x} + \nu \nabla^2 u \quad (2)$$

$$v \frac{\partial v}{\partial x} + v \frac{\partial v}{\partial y} = -\frac{1}{\rho} \frac{\partial P}{\partial y} + \nu \nabla^2 v \quad (3)$$

$$u \frac{\partial T}{\partial x} + v \frac{\partial T}{\partial y} = \alpha \nabla^2 T \quad (4)$$

where  $x$  and  $y$  are the cartesian coordinates (m),  $u$  and  $v$  are the velocity components in  $x$  and  $y$  directions (m/s),  $\rho$  is the specific mass of the fluid (kg/m<sup>3</sup>),  $\nu$  is the kinematic viscosity of the fluid (m<sup>2</sup>/s),  $\alpha$  is the thermal diffusivity of the fluid (m<sup>2</sup>/s),  $T$  is the temperature (°C or K), and  $\nabla^2$  means  $\nabla^2 = \partial/\partial x^2 + \partial/\partial y^2$ .

For solving Eq. (1)-(4) numerically, the dimensionless coordinates, velocities, temperature, and pressure are obtained from Eq. (5a)-(5d):

$$(\tilde{x}, \tilde{y}) = \frac{(x, y)}{D_0} \quad (5a)$$

$$(\tilde{u}, \tilde{v}) = \frac{(u, v)}{U_\infty} \quad (5b)$$

$$\tilde{T} = \frac{T - T_\infty}{T_s - T_\infty} \quad (5c)$$

$$\tilde{P} = \frac{P}{\rho U_\infty^2} \quad (5d)$$

In the equations above the symbol ( $\sim$ ) indicates dimensionless variables;  $U_\infty$  is the free-stream velocity (m/s),  $T_\infty$  is the free-stream temperature (°C or K),  $T_s$  is the temperature of the square cylinder (°C or K), and  $P$  is pressure (Pa). Then, the resulting dimensionless equations can be written as:

$$\frac{\partial \tilde{u}}{\partial \tilde{x}} + \frac{\partial \tilde{v}}{\partial \tilde{y}} = 0 \quad (6)$$

$$\tilde{u} \frac{\partial \tilde{u}}{\partial \tilde{x}} + \tilde{v} \frac{\partial \tilde{u}}{\partial \tilde{y}} = -\frac{\partial \tilde{P}}{\partial \tilde{x}} + \frac{1}{\text{Re}_{D_0}} \nabla^2 \tilde{u} \quad (7)$$

$$\tilde{v} \frac{\partial \tilde{v}}{\partial \tilde{x}} + \tilde{v} \frac{\partial \tilde{v}}{\partial \tilde{y}} = -\frac{\partial \tilde{P}}{\partial \tilde{y}} + \frac{1}{\text{Re}_{D_0}} \nabla^2 \tilde{v} \quad (8)$$

$$\tilde{u} \frac{\partial \tilde{T}}{\partial \tilde{x}} + \tilde{v} \frac{\partial \tilde{T}}{\partial \tilde{y}} = \frac{1}{\text{Re}_{D_0} \text{Pr}} \nabla^2 \tilde{T} \quad (9)$$

$Pr$  and  $\text{Re}_{D_0}$  are dimensionless parameters, Prandtl and Reynolds numbers, respectively, which are defined by:

$$\text{Pr} = \frac{\nu}{\alpha} \quad (10a)$$

$$\text{Re}_{D_0} = \frac{\rho U_\infty D_0}{\mu} \quad (10b)$$

where  $\mu$  is the kinematic viscosity (kg/ms), and  $D_0$  is the characteristic length used to compute the Reynolds number (m).

The boundary conditions as function of dimensionless variables are observed in Fig. 1. The fluid dynamics boundary conditions are no slip and no penetration on the obstacle surfaces, free slip and no penetration on the symmetry surfaces, prescribed velocity ( $\tilde{u} = 1$ ) on the inlet surface, and  $\partial(\tilde{u}, \tilde{v})/\partial \tilde{x} = 0$  on the outlet surface. Concerning to the thermal boundary conditions, they are prescribed temperature on the obstacle surfaces ( $\tilde{T} = 1$ ) and on the inlet plane of computational domain ( $\tilde{T} = 0$ ). The remaining boundaries of the computational domain are adiabatic.

To obtain the optimal arrangement of square bluff-bodies, the overall heat transfer rate between the cylinder and the surrounding fluids is fixed as objective function, which in its dimensionless form is given by the following expression:

$$\tilde{q} = \frac{q'}{k(T_s - T_\infty)} \quad (11)$$

where  $q'$  is the heat transfer rate integrated over the surface of one cylinder between the obstacle and the surrounding fluid (W/m), and  $k$  is the thermal conductivity (W/mK).

Equation (6)-(9) were solved by using a CFD package based on rectangular finite volume (Fluent, 2007). The solver is pressure based (coupled 2<sup>nd</sup> order for pressure and Power-law scheme for momentum and energy). The grid is stretched with more refined volumes near the surfaces of the obstacle. The appropriate mesh size dimension was determined by successive refinements until the criterion  $|(Nu^i - Nu^{i+1})| \leq 5 \times 10^{-3}$  was satisfied, where  $Nu^i$  is the spatial averaged Nusselt number using the current mesh and  $Nu^{i+1}$  is the spatial averaged Nusselt number correspondent to the next mesh.

Table 1 shows the attainment of grid independence for flows with  $Re = 100$  and  $Pr = 0.7$ . The grid independent results agree with those presented in Sahu *et al.* (2009) and Sharma and Eswaran (2004), within 1.01% and 0.54%, respectively. Convergence was achieved when the following maximal residual were reached:  $10^{-4}$  for mass and momentum equations and  $10^{-8}$  for energy equation. Double precision was used for all numerical simulations.

Table 1. Grid independence as function of Nusselt number for a flow with  $Re = 100$  and  $Pr = 0.7$

Number of elements	Nusselt number	$ (Nu^i - Nu^{i+1})  \leq 5 \times 10^{-3}$
36175	4,3877	
52380	4,2782	$2.50 \times 10^{-2}$
105910	4,1882	$2.10 \times 10^{-2}$
143900	4,1385	$1.19 \times 10^{-2}$
171848	4,1058	$7.90 \times 10^{-3}$
207600	4,0848	$5.11 \times 10^{-3}$
324375	4,0661	$4.58 \times 10^{-3}$

For validation of the code it was simulated steady, incompressible, forced convection flows at laminar regime for various Prandtl numbers,  $Pr = 1, 10$  and  $20$ , and Reynolds numbers of  $Re = 60$  and  $160$ . The local Nusselt numbers for the top half of the square cylinder are compared with the results of Sahu *et al.* (2009), as can be seen in Fig. 2a for  $Re = 60$  and Fig. 2b for  $Re = 160$ . One observes that all results agree within 4%. The worst situation occurs for a flow with  $Pr = 20$  and  $Re = 160$ .

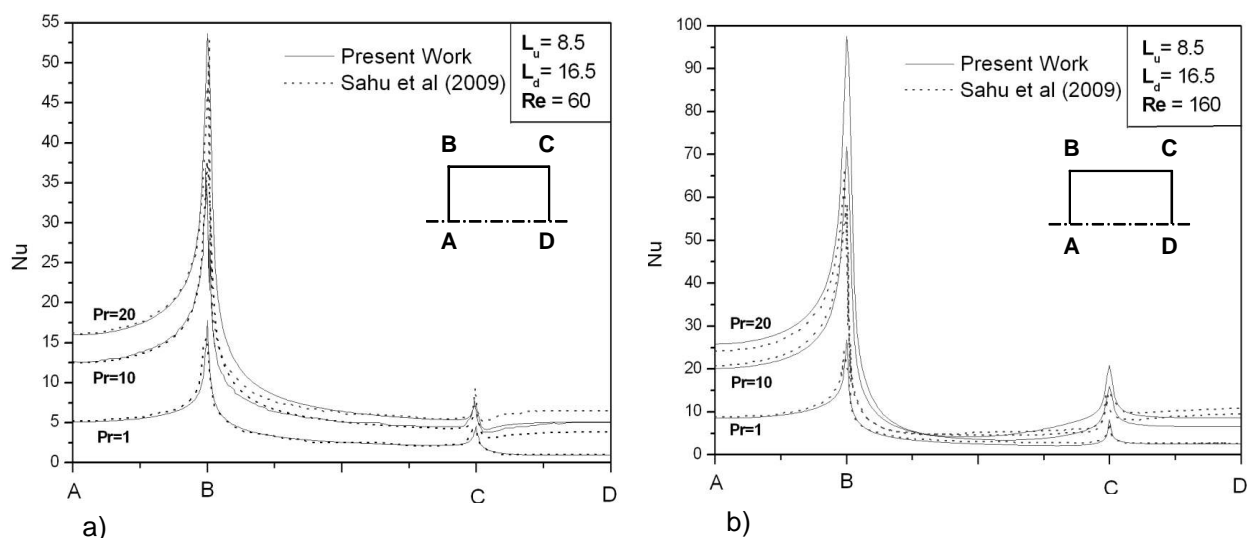


Figure 2. Local Nusselt number obtained from the present code and that presented in Sahu *et al.* (2009) for flow with various Prandtl numbers,  $Pr = 1, 10$  and  $20$ , and a fixed Reynolds number – a)  $Re = 60$  and b)  $Re = 160$

### 3. RESULTS

The flow and temperature fields were simulated in a large number of configurations to determine the effect of spacing on heat transfer rate. For the achievement of this objective, the bluff-bodies arrange is submitted to a global restriction, given by the ratio  $H/D_0$ , and to one degree of freedom, which is the distance between the square cylinders ( $s_0$ ). For all geometric configurations it was simulated various Prandtl numbers,  $Pr = 0.1, 0.72, 1.0$  and  $10.0$ , and Reynolds numbers,  $Re = 60, 100$  and  $160$ , with the purpose to evaluate the behavior of heat transfer rate from the obstacles to surrounding flow as function of these dimensionless parameters.

Figure 3 shows the dimensionless heat transfer rate ( $\bar{q}$ ) as function of the distance between the square cylinders ( $\tilde{s}_0$ ) for various Reynolds numbers,  $Re = 60, 100$  and  $160$ , and a fixed Prandtl number. Figure 3a presents this evaluation for a Prandtl number of  $Pr = 0.1$ . One observes that there is an optimal geometric configuration for all evaluated Reynolds numbers. These optimal configurations, for each Reynolds number, do not correspond to the highest or lowest space between the square cylinders ( $\tilde{s}_0$ ). In other words, the optimal geometry is not obtained by the insertion of the maximum or the minimum number of obstacles in a fixed space,  $H$ . It is also investigated the behavior of the optimal non-dimensional distance between square cylinders ( $\tilde{s}_{0,opt}$ ) as function of Reynolds number ( $Re$ ),  $\tilde{s}_{0,opt}$  decreases as Reynolds number increases. This same behavior was previously shown in Bello-Ochende and Bejan (2005) for a cross-flow over circular cylinders. In that study, the optimal geometry is obtained as function of Bejan number,  $Be$ , instead of Reynolds number,  $Re$ , as presented here. Since both dimensionless parameters,  $Be$  and  $Re$ , has a similar influence for the determination of an optimal assembly, a comparison of the behavior of optimal distance between square and circular cylinders as function of Reynolds and Bejan numbers, respectively, is suitable.

In Figure 3b, the dimensionless heat transfer rate ( $\bar{q}$ ) as function of the distance between the square cylinders ( $\tilde{s}_0$ ) for a fixed Prandtl number  $Pr = 0.72$  is presented. In comparison with the previous case,  $Pr = 0.1$ , the optimal distances between the square cylinders for all Reynolds numbers has decreased significantly, but it has not yet decreased until the minimal distance ( $\tilde{s}_{0,opt} \neq \tilde{s}_{0,min}$ ) for flows with  $Re = 60$  and  $100$ . Except for a flow with  $Re = 160$ , where the optimal dimensionless distance between the square cylinders is minimal,  $\tilde{s}_{0,opt} = \tilde{s}_{0,min}$ . In addition, for  $Pr = 0.72$  the optimal distance between the square obstacles  $\tilde{s}_{0,opt}$ , as well as for  $Pr = 0.1$ , decreases as Reynolds number increases.

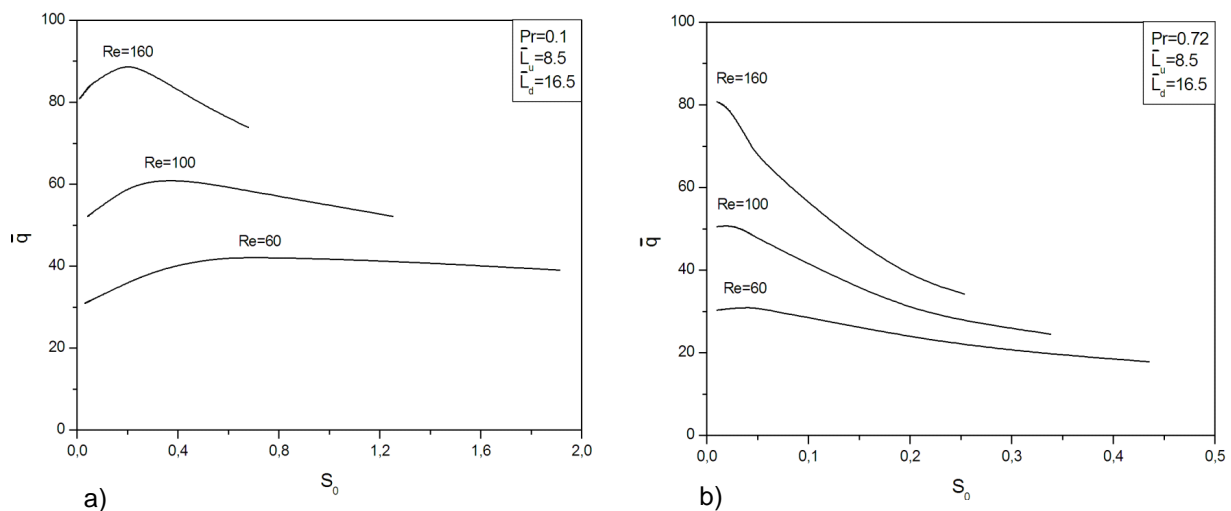


Figure 3. The optimization of dimensionless heat transfer rate ( $\bar{q}$ ) as function of the dimensionless distance between the square cylinders ( $\tilde{s}_0$ ) for various Reynolds numbers,  $Re = 60, 100$  and  $160$ , and Prandtl numbers: a)  $Pr = 0.1$  and b)  $Pr = 0.72$

For a better understanding of the thermal behavior as function of the dimensionless distance between square cylinders,  $\tilde{s}_0$ , the temperature distribution for three different arrangements and a flow with  $Re = 60$  and  $Pr = 0.72$ , is presented in Fig. 4. The first one, Fig. 4a, represents the largest distance between the square cylinders. The second one, Fig. 4b, represents an intermediate distance and the last one, Fig. 4c, represents the shortest distance between the square cylinders. The decrease of the dimensionless distance between the square cylinders, from Fig. 4a to Fig. 4b, led to an increasing of the heat exchange between the obstacle and the surrounding flow. This fact is related with the increase of the temperature gradients around the obstacles. Nevertheless, from distances lower than  $\tilde{s}_0 = \tilde{s}_{0,opt} = 0.04$ , as illustrated in Fig. 4c, the interaction of thermal boundary layers happens such that diffusion dominates the heat transfer process, consequently, the heat exchange rate between the square cylinders and the surrounding flow drops down again. Therefore, there is one distance between square cylinders where the increasing of heat exchange area is balanced by the interaction of thermal boundary layers, attempting to an optimal configuration. For this analyzed case, this balance happens for the distance between the square cylinders of  $\tilde{s}_0 = 0.04$ .

When the Prandtl number increases, not only the dimensionless optimal distance between square cylinders,  $\tilde{s}_{0,opt}$ , but also the dimensionless optimal heat transfer rate between the arrange and the surrounding flow,  $\tilde{q}_{opt}$ , decreases, for a fixed Reynolds number, as illustrated in Fig. 3a and 3b. This fact is linked with the increasing of thermal boundary layer for higher Prandtl numbers. This tendency is corroborated when higher Prandtl numbers are evaluated,  $Pr = 1.0$  and  $10.0$ , shown in Fig. 5a and 5b, respectively.

For a Prandtl number of  $Pr = 1$ , Fig. 5a, the optimal distance between the square cylinders corresponds to the minimal one, except for  $Re = 60$ . For a Prandtl number of  $Pr = 10.0$ , Fig. 5b, the optimal distance between the square cylinders is the minimal for all Reynolds numbers.

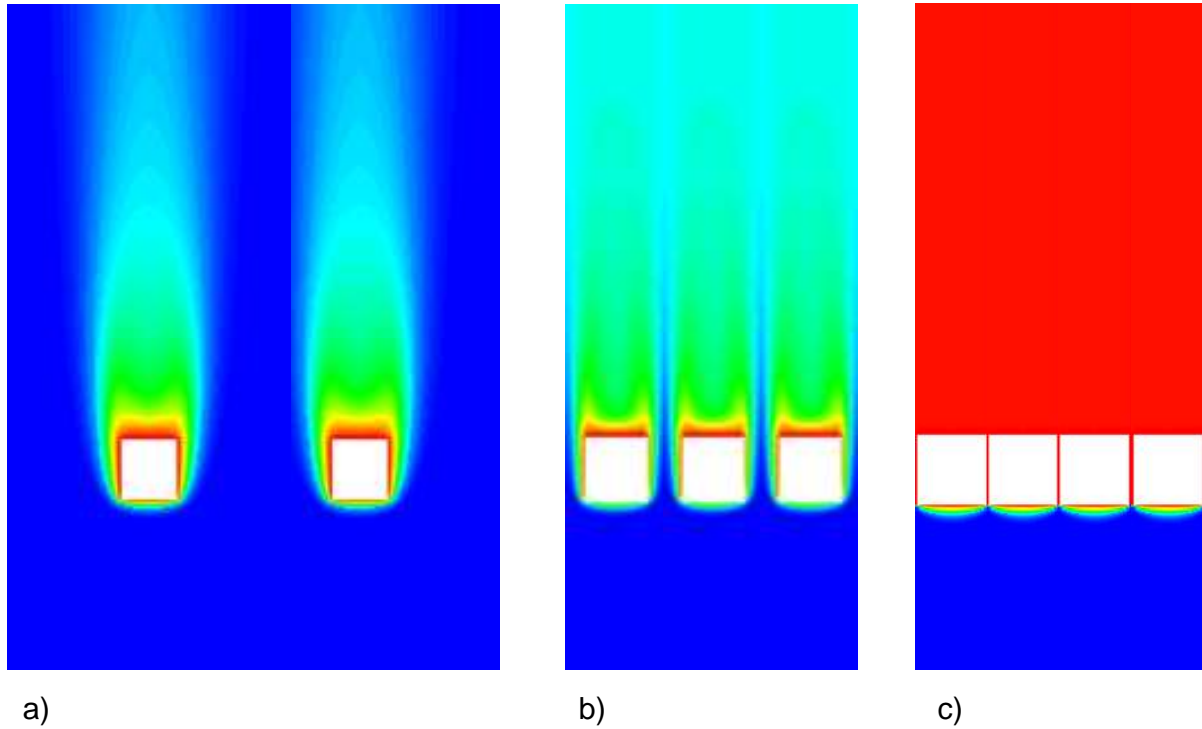


Figure 4. Temperature distribution as function of the spacing between square cylinders ( $\tilde{s}_0$ ): a) long distance; b) intermediate distance (optimal configuration) and c) short distance

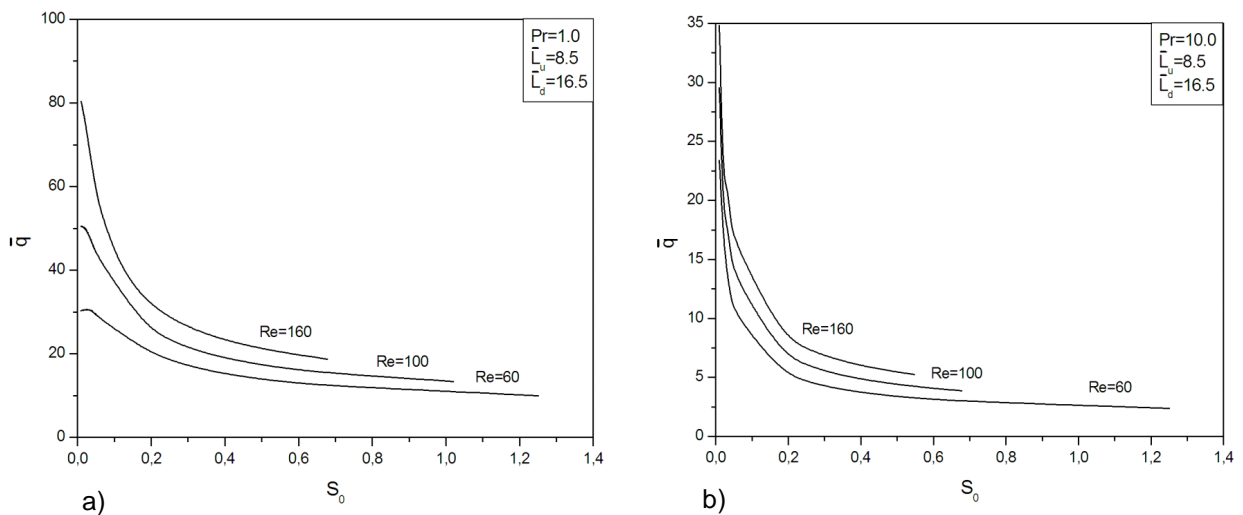


Figure 5. Optimization of dimensionless heat transfer rate ( $\tilde{q}$ ) as function of the dimensionless distance between the square cylinders ( $\tilde{s}_0$ ) for various Reynolds numbers,  $Re = 60, 100$  and  $160$ , and Prandtl numbers: a)  $Pr = 1.0$  and b)  $Pr = 10.0$

Figure 6 presents the dimensionless optimal distance between the square cylinders ( $\tilde{s}_{0,opt}$ ) and the dimensionless optimal heat transfer rate ( $\tilde{q}_{opt}$ ) as function of Reynolds number. Since these variables have different magnitude orders

they will be presented in the graphs with the following manipulation  $10 \times \tilde{s}_{0,opt}$  and  $\tilde{q}_{opt}/10$ , respectively. In Fig 5a and 5b these variables are evaluated for fixed Prandtl numbers of  $Pr = 0.1$  and  $Pr = 0.72$ , respectively. For both Prandtl numbers,  $\tilde{s}_{0,opt}$  decreases with the increasing of Reynolds number, while  $\tilde{q}_{opt}$  has an opposite behavior. It is also observed that the dimensionless optimal heat transfer rate ( $\tilde{q}_{opt}$ ) increases linearly with the increasing of Reynolds number. Nevertheless, the rate of dimensionless optimal distance between the square cylinders ( $\tilde{s}_{0,opt}$ ) has a more steeped decline for lower Reynolds ( $60 \leq Re \leq 100$ ) than for higher Reynolds ( $100 \leq Re \leq 160$ ).

Figure 7 shows the dimensionless optimal distance between the square cylinders ( $\tilde{s}_{0,opt}$ ) and the dimensionless optimal heat transfer rate ( $\tilde{q}_{opt}$ ) as function of Prandtl number, for Reynolds numbers of  $Re = 60$  and  $Re = 160$ , Fig. 7a and 7b, respectively. For simplification, we will not show the dimensionless optimal variables as function of Prandtl number for  $Re = 100$ . The dimensionless optimal heat transfer rate ( $\tilde{q}_{opt}$ ) decreases with the increasing of the Reynolds number. Concerning the dimensionless optimal spacing between square cylinders ( $\tilde{s}_{0,opt}$ ) a similar behavior is found. One also observes that for lower Prandtl numbers,  $Pr \leq 1$ , specially for Reynolds number of  $Re = 60$ , there are a steep decline of the dimensionless optimal spacing between square cylinders ( $\tilde{s}_{0,opt}$ ) as function of Prandtl number, as can be seen in Fig 7a. This fact is not so intense for  $Re = 160$  since the increase of Reynolds number decreases the dimensionless optimal distance between square cylinders ( $\tilde{s}_{0,opt}$ ). Then, even for lower Prandtl numbers the values of  $\tilde{s}_{0,opt}$  is near to the minimum. When Prandtl number is  $Pr > 1$ ,  $\tilde{s}_{0,opt}$  is quasi-independent of Prandtl number. With the significant increase of thermal boundary layer the sole alternative to increase the heat exchange between the square cylinders arrange and the surrounding flow is to increase the area of heat exchange.

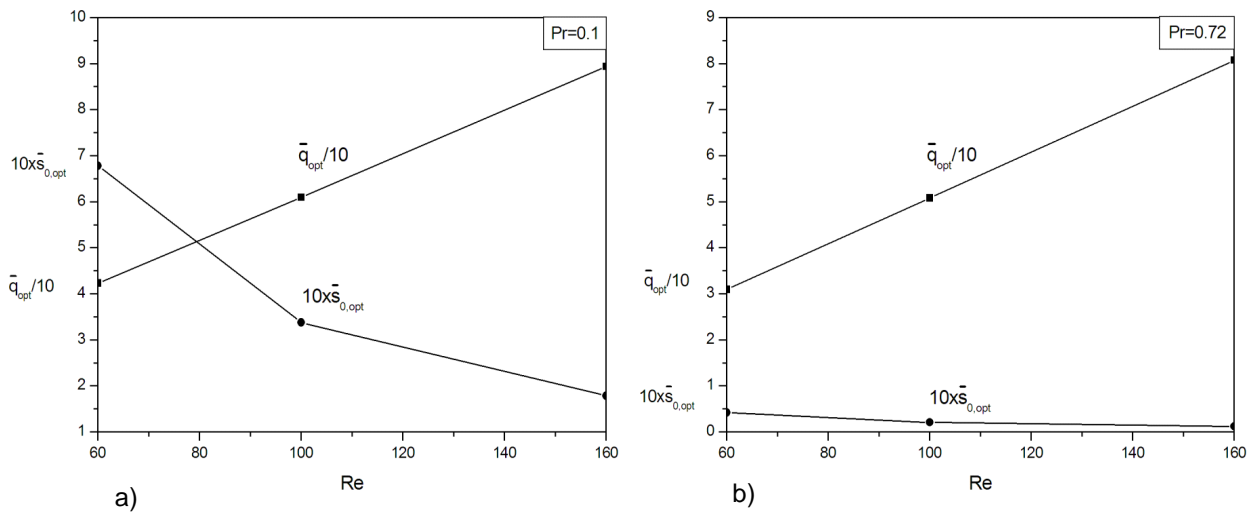


Figure 6. Dimensionless optimal heat transfer rate ( $\tilde{q}_{opt}$ ) and dimensionless optimal spacing between square cylinders ( $\tilde{s}_{0,opt}$ ) as function of Reynolds numbers for Prandtl numbers: a)  $Pr = 0.1$  and b)  $Pr = 0.72$

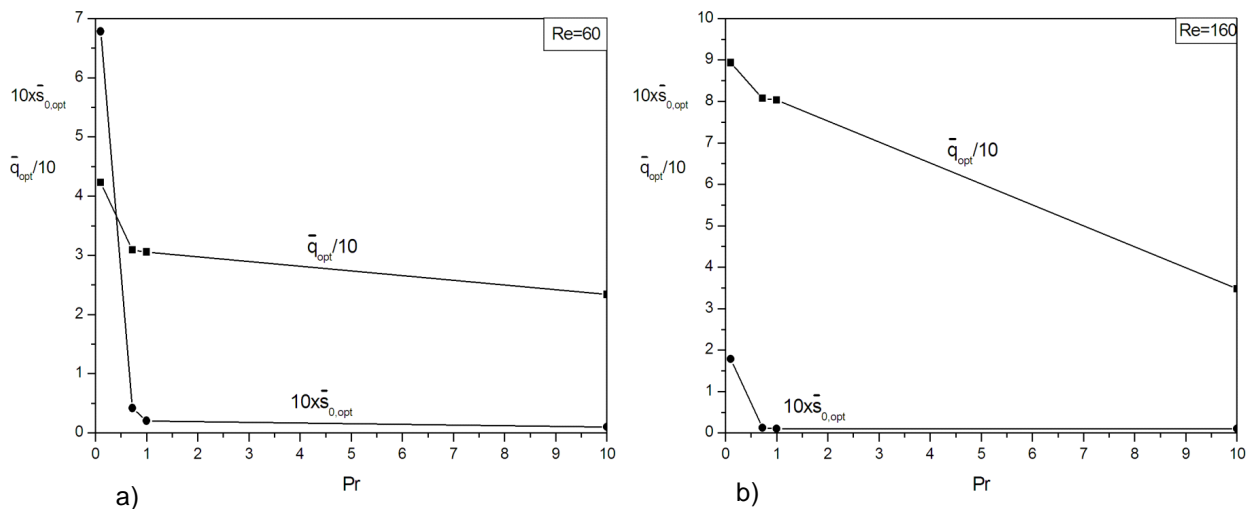


Figure 7. Dimensionless optimal heat transfer rate ( $\tilde{q}_{opt}$ ) and dimensionless optimal spacing between square cylinders ( $\tilde{s}_{0,opt}$ ) as function of Prandtl numbers for Reynolds numbers: a)  $Re = 60$  and b)  $Re = 160$

#### 4. CONCLUSION

The present work presented a numerical study of the maximization of heat transfer rate from an assembly of square cylinders to a surrounding flow employing Constructal theory. Various square cylinder assemblies were analyzed to select the best spacing between square cylinders that optimizes the heat transfer rate. The flow system was submitted to one global restriction ( $H/D_0$ ) and one degree of freedom ( $\tilde{s}_0$ ) was optimized. For all geometric configurations it was performed simulations with various Prandtl,  $Pr = 0.1, 0.72, 1.0$  and  $10.0$ , and Reynolds numbers,  $Re = 60, 100$  and  $160$ , to investigate the influence of these dimensionless parameters in the optimization of assembly geometry.

When the dimensionless heat transfer rate ( $\tilde{q}$ ) was obtained as function of the dimensionless distance between the square cylinders ( $\tilde{s}_0$ ) it was observed that for lower Prandtl numbers, especially for  $Pr = 0.1$ , the optimal configuration of the assembly is achieved when the cylinders are brought close enough so that their thermal boundary layers just touch. However, for higher Prandtl numbers,  $Pr$ , especially for  $Pr = 10.0$ , the optimal configuration is achieved for minimal distances between the obstacles by the increasing of the heat exchange area, since the thermal boundary layer increases significantly allowing only diffusion heat transfer between the obstacles and the surrounding flow. Therefore, there is one distance between square cylinders where the increasing of heat exchange area is balanced by the interaction of thermal boundary layers, so that one optimal configuration is achieved.

The dimensionless optimal distance between square cylinders,  $\tilde{s}_{0,opt}$ , decreased with the increasing of Reynolds number for a fixed Prandtl number, except for Prandtl numbers higher than  $Pr > 1$ , where the dimensionless optimal distance between square cylinders was independent of the Reynolds number. It also decreased with the increasing of Prandtl number,  $Pr$ , for a fixed Reynolds number.

The dimensionless heat transfer rate,  $\tilde{q}_{opt}$ , increased with the increasing of Reynolds number,  $Re$ , for a fixed Prandtl number,  $Pr$ , and decreased with the increasing to Prandtl number,  $Pr$ , for a fixed Reynolds number,  $Re$ .

It is also worth to note that the dimensionless optimal distance between the square cylinders,  $\tilde{s}_{0,opt}$ , and the dimensionless heat transfer rate,  $\tilde{q}_{opt}$ , as function of Reynolds number presented a similar behavior to those presented by Bello-Ochende and Bejan (2005) for cross-flows over assemblies of circular cylinders.

#### 5. ACKNOWLEDGEMENTS

E.D. dos Santos thanks CAPES by his doctorate scholarship. L.A.O. Rocha thanks CNPq for research grant.

#### 6. REFERENCES

- Bejan, A., 1994, "Convection heat transfer", Jhon Wiley & Sons, Durhan, North Caroline, USA, 623 p.
- Bejan, A., 1997, "Advanced engineering thermodynamics, Willey, New York, USA.
- Bejan, A., 2000, "Shape and structure from engineering to nature", Cambridge University Press, Cambridge, UK.
- Bejan, A., Lorente, S., 2006, "Constructal theory of generation of configuration in nature and engineering", Journal of Applied Physics, Vol. 100, pp. 041 – 301.
- Bejan, A., Lorente, S., 2008, "Design with Constructal theory", Willey, Hoboken.
- Bello-Ochende, T., Bejan, A., 2005, "Constructal multi-scale cylinders in cross-flow", International Journal of Heat and Mass Transfer, Vol. 48, pp. 1373 – 1383.
- Bello-Ochende, T., Lienbenberg, L., Malan, A.G., Bejan, A., Meyer, J.P., 2007a, "Constructal conjugate heat transfer in three-dimensional cooling channels", Journal of Enhanced Heat Transfer, Vol. 14, pp. 279-293.
- Bello-Ochende, T., Lienbenberg, L., Malan, A.G., Bejan, A., Meyer, J.P., 2009, "Constructal ducts with wrinkled entrances", International Journal of Heat and Mass Transfer, doi:10.1016/j.ijheatmasstransfer.2009.03.014.
- Bello-Ochende, T., Lienbenberg, L., Bejan, A., 2007b, "Constructal cooling channels for micro-channel heat sinks", International Journal of Heat and Mass Transfer, Vol. 50, pp. 4141 – 4150.
- Fluent (version 6.3.16), ANSYS, Inc., 2007.
- Sahu, A. K., Chhabra, R. P., Eswaran, V., 2009, "Effects of Reynolds and Prandtl numbers on heat transfer from a square cylinder in the unsteady flow regime", International Journal of Heat and Mass Transfer, Vol. 52, pp. 839 – 850.
- Sharma, A., Eswaran, V., 2004, "Heat and fluid flow across a square cylinder in the twodimensional laminar flow regime", Numer. Heat Transfer A 45 (3), pp. 247 – 269.

#### 7. RESPONSIBILITY NOTICE

The author(s) is (are) the only responsible for the printed material included in this paper.